Journal of Applied Electrochemistry **30**: 1313–1316, 2000.

Short communication

Magnetic properties of electrodeposited nickel–manganese alloys: Effect of Ni/Mn bath ratio

A. STEPHEN[1], M.V. ANANTH[2], V. RAVICHANDRAN[1] and B.R.V. NARASHIMAN[3]
[1]*Materials Science Centre, Department of Nuclear Physics, University of Madras, Guindy Campus, Chennai – 600 025, India*
[2]*Central Electrochemical Research Institute – Madras Unit, CSIR Complex, Chennai – 600 113, India*
[3]*National Metallurgical Laboratory – Madras Centre, CSIR Complex, Chennai – 600 113, India*

Received 17 December 1998; accepted in revised form 28 June 2000

Key words: alloys, electrodeposition, magnetic properties, Ni–Mn binary system

1. Introduction

Electrodeposition is an important cost-effective, yet fast, route for preparing porosity-free pure metals and alloys as films or in bulk form. The deposited materials exhibit grain sizes less than 100 nm [1]. It is well established that such nanostructured materials have enhanced physical properties due to the increased volume fractions of grain boundaries. For magnetic materials considerable change is expected in their magnetic behaviour when the grain size approaches the domain wall thickness.

The magnetic properties of electrodeposited alloys of nickel with several elements like iron, cobalt and phosphorous have been previously investigated [2, 3]. However, the magnetic behaviour of electrodeposited Ni–Mn alloys has not been studied, even though results on certain magnetic properties of thermally prepared Ni–Mn are available [4, 5]. The magnetic structure with neighbourhood interactions between ferromagnetic Ni and anti-ferromagnetic Mn, coupled with the composition-driven order–disorder characteristics, makes Ni–Mn an interesting system. Thus, data on the magnetic parameters like saturation magnetization and coercivity of Ni–Mn electrodeposits with different compositions are useful in assessing its application potential. The effect of structural disorder and microstructural features on these parameters are also discussed.

2. Experimental details

Ni–Mn alloys were electrodeposited on stainless steel substrates from simple sulphate baths with a wide range of composition by varying the Ni/Mn salt ratio [6]. All depositions were carried out in a 1 dm^3 rectangular cell at a current density of 30 mA cm^{-2} at room temperature. Bagged graphite blocks (5 cm × 9 cm) constituted the insoluble anodes. Stainless steel plates of size 2.8 cm × 7 cm × 0.75 cm were used after surface pretreatments such as mechanical polishing, buffing, degreasing with benzene followed by acetone and washing with detergent followed by a final washing in distilled water. The edges of the panels were masked with lacquer. An area of 4 cm × 5 cm on both sides was left exposed to the electrolyte during plating.

Efforts were initially made to study the preparation of practical deposits obtained from solution of pH 3. No attempt was made to take into consideration pH changes during deposition. The deposited alloys were mechanically removed from the substrate and studied.

The microstructures were examined using a Leica Reichert Polyvar metallurgical optical microscope under bright field. The magnetic hysteresis experiments on the deposits were performed using a PAR EGsG vibrating sample magnetometer. The X-ray diffraction of the deposits was carried out using a Guinier type camera employing a focusing geometry and a solid-state detector. The radiation used was CuK_{α_1}. The chemical composition of the alloy was determined using standard analytical procedures wherein nickel was estimated by gravimetric analysis as Ni–DMG complex and manganese by spectrophotometric analysis.

3. Results and discussion

The X-ray diffractogram of a typical deposit is as shown in Figure 1. It indicates a single highly crystalline f.c.c.

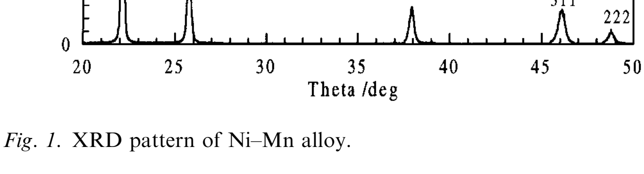

Fig. 1. XRD pattern of Ni–Mn alloy.

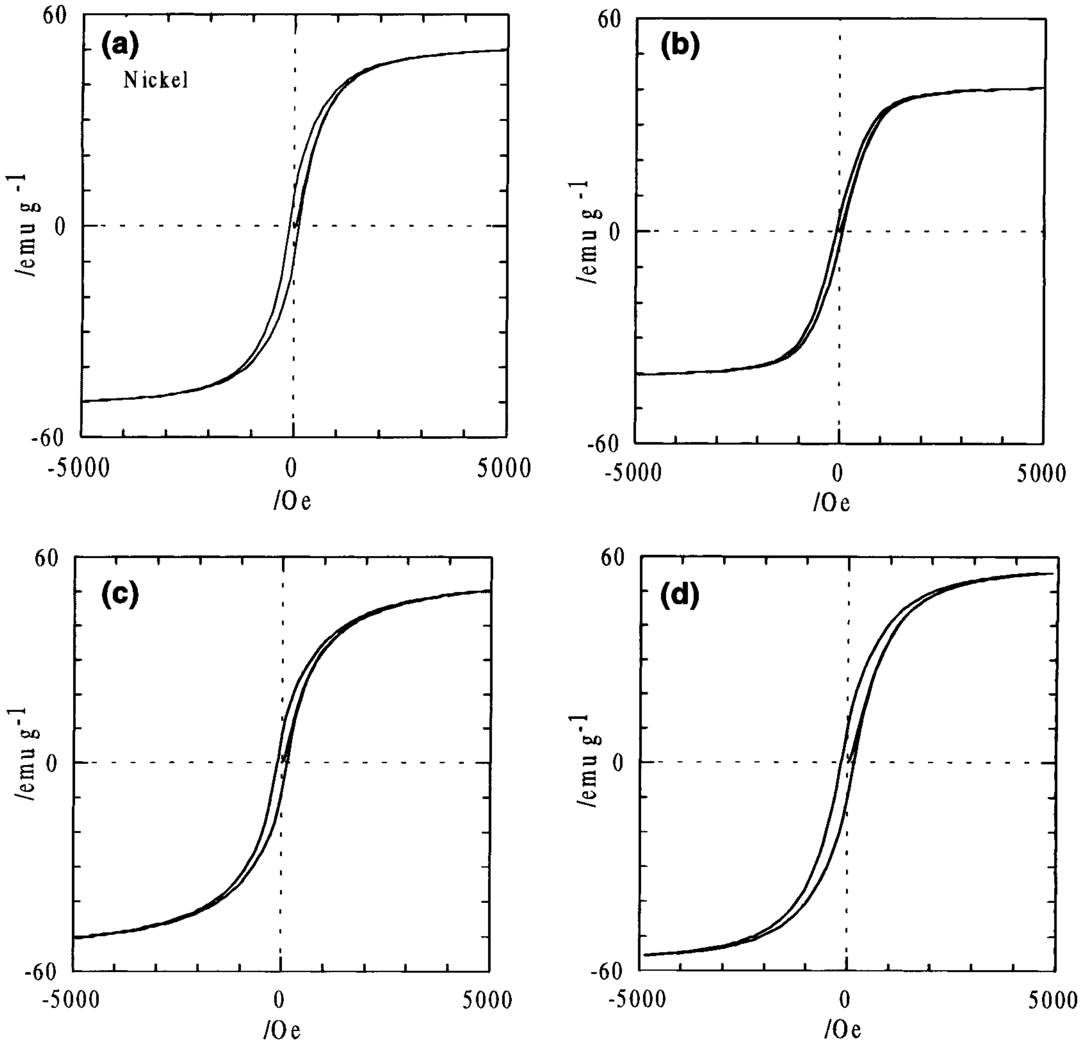

Fig. 2. Hysteresis curves for (a) electrodeposited nickel, (b) Ni20–Mn150, (c) Ni100–Mn150 and (d) Ni150–Mn25 samples.

phase with a lattice spacing of 3.524 Å (i.e., 352.4 pm). The average size of the crystallite grains was determined by extracting the size-dependent component from the broadened diffraction profile and carrying out a Fourier analysis [7]. The crystallite size was typically 30 nm. The alloy deposits therefore possess a nanocrystalline structure.

Figure 2 shows the hysteresis loops obtained for some representative samples with high and low Mn concentration. The hysteresis parameters, namely saturation

Table 1. Magnetic properties of electrodeposited Ni–Mn alloys

Deposit	Bath composition/g dm^{-3}		Ni composition /at %	M /emu g^{-1}	H_C /Oe	R /emu g^{-1}
	$NiSO_4 \cdot 6H_2O$	$MnSO_4 \cdot H_2O$				
1	10	150	69.2	24.31	61.05	2.00
2	20	150	71.1	40.76	77.65	3.00
3	40	150	72.4	45.90	86.82	4.30
4	60	150	73.6	46.32	94.85	4.48
5	80	150	74.8	48.13	133.0	8.56
6	100	150	76.2	50.40	115.0	8.50
7	120	150	77.3	50.55	111.1	6.50
8	140	150	78.4	51.44	108.6	8.75
9	150	150	79.0	51.81	91.84	4.30
10	150	100	79.6	52.20	98.10	6.04
11	150	75	80.7	51.36	88.40	5.88
12	150	50	82.4	53.99	86.85	7.41
13	150	25	92.1	54.24	151.9	10.1
14	150	10	97.4	55.26	116.0	9.62
15	150	–	100	50.11	94.6	10.3

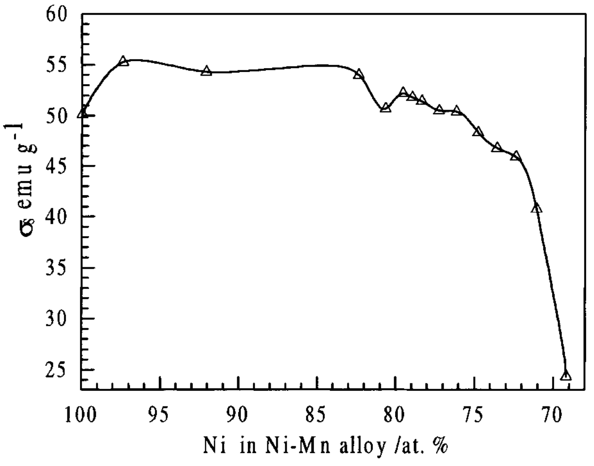

Fig. 3. Saturation against Ni (at %) in Ni–Mn alloy.

magnetisation (σ_s), coercivity (H_c) and remanence (R) for all the deposits, are shown tabulated against their Ni atomic percentage compositions in Table 1. The bath composition employed for each deposit is also shown for reference. The Ni–Mn prefers to deposit as Ni-rich (a minimum of about 70 at % of Ni) alloys irrespective of the bath composition. This is consistent with the known preference for the Ni_3Mn phase by the Ni–Mn solid solution [8]. The X-ray diffraction peaks also signify a f.c.c. phase close to that of Ni_3Mn. Therefore, it is more meaningful to discuss the magnetic behaviour as a function of Ni atomic percent.

Figure 3 shows the variation of saturation magnetisation with nickel concentration. The general decreasing trend in σ_s with increasing Mn can be understood as a consequence of the suppression of the ferromagnetic character of nickel. Interestingly, σ_s does not vary much for the first 15 at % of Mn addition whereas it decreases rapidly over the next 15%. In fact, σ_s at very low Mn concentration is even higher than that of electrodeposited pure nickel at 50 emu $\cdot$ g^{-1} . The overall behaviour of σ_s resembles the trend reported in the literature [9] for ordered Ni_3Mn phase for the composition band of 70 to 80 at % Ni and that for the disordered phase for Ni greater than 80%. The saturation magnetization is not expected to have any pronounced dependence on the grain size [10].

The coercivity and remanence show wide fluctuations in the given compositional range, with high values for certain deposits. The pinning of domain wall energy by a second phase in the ferromagnetic matrix, dislocations and/or internal stress fields, as well as anisotropy due to surface and particle shape, are important factors that can increase the coercivity [11]. The optical micrographs in Figure 4 exhibit pyramidal growth in the surface morphology suggesting that the surface anisotropy in these deposits might be a significant contributor to the

▶

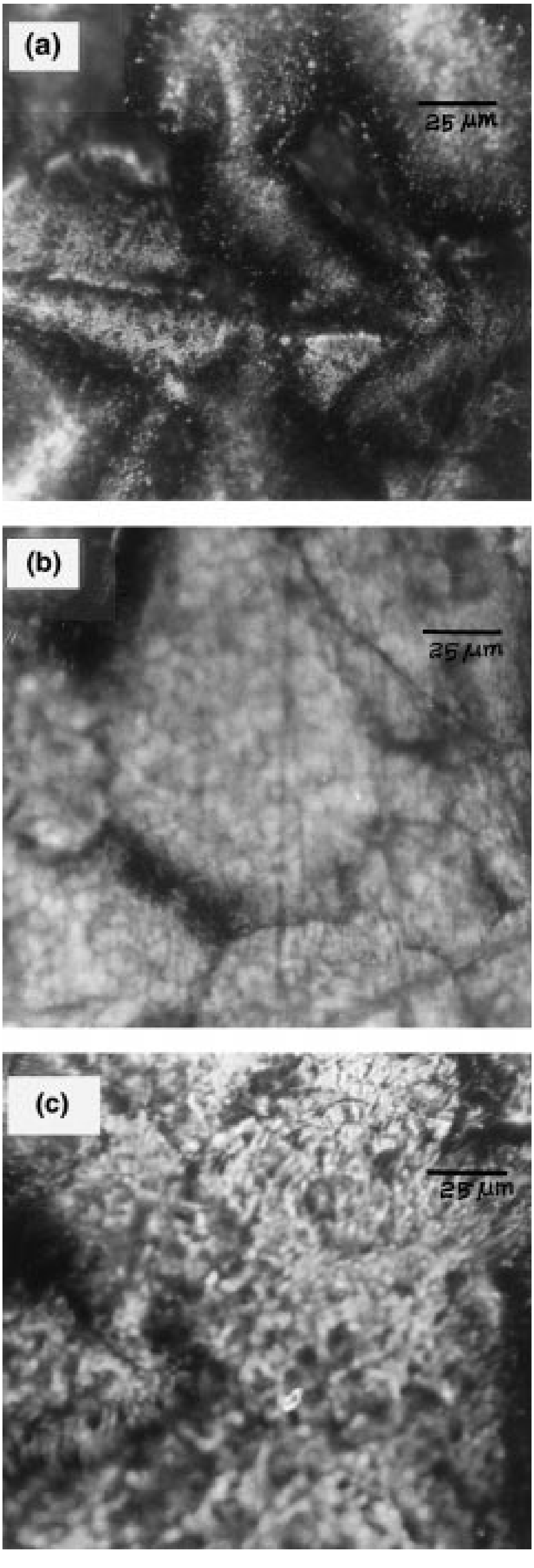

Fig. 4. Bright field optical micrographs of electrodeposits from different bath compositions at a current density of 30 mA cm^{-2}. (a) Ni80–Mn150, (b) Ni120–Mn150 and (c) Ni150–Mn75.

high coercivity values of about 130 Oe. Since the deposits appear textured along the easy magnetic direction of ⟨111⟩ for nickel, as shown in Figure 1, stress is less likely to have been a contributor. However, the crystallite size of about 30 nm for the grains in the deposit is much smaller than the domain wall thickness for nickel; the large coercivities can also be explained by a single-domain theory [12]. An increase in coercivity with decreasing grain size has been reported for electrodeposited Ni–P [13].

4. Conclusion

Electrodeposition produces Ni–Mn alloys in a narrow composition band for widely varying Ni/Mn, bath salt ratios. These deposits probably exist as ordered, as well as disordered, Ni_3Mn phases. The alloys exhibit enhanced magnetic coercivity and remanance over the bulk nickel and the magnetisation varies as a function of manganese concentration. It appears that, under controlled conditions, a material with unusual magnetic properties for specific applications can be achieved by electrodeposition.

Acknowledgement

This work was supported by the SAP–UGC program of the Government of India.

References

1. A. Stephen, T. Nagarajan and M.V. Ananth, *Mat. Sci. Eng. B* **55** (1998) 184.
2. K.I. Arai, H.W. Kang, and K. Ishiyama, *IEEE Trans. Magnetics* **27** (1991) 4906.
3. M. Matsubara and A. Yamada, *J. Electrochem. Soc.* **141** (1994) 2386.
4. A.R. Ali, Z.M. Farid and E. Takla, *Phys. Stat. Sol. (a)* **129** (1992) 87.
5. T. Sato, T. Ando, T. Oku and S. Morimoto, *J. Mag. Mag. Mater.* **140–144** (1995) 1973.
6. A. Stephen, M. Ilango, T. Nagarajan and M.V. Ananth, *Trans. IMF.* **76** (1998) 111.
7. D. Balzar, *J. Appl. Cryst.* **25** (1992) 559.
8. T.B. Massalshi, 'Binary Alloy Phase Diagrams', Vol. 3 ASM, Metals Park, OH (1992) p. 2582.
9. S.K. Sidorov and A.V. Doroshenko, *Phys. Stat. Sol.* **16** (1966) 737.
10. B. Szpunar, U. Erb, G. Palumbo, K.T. Aust and L.J. Lewis, *Phy. Rev. B.* **53** (1996) 5547.
11. D. Jiles, *in* 'Introduction to Magnetism and Magnetic Materials', Chapman Hall, London (1991) p. 146.
12. H. Kronmuller and H.R. Hilzinger, *Int. J. Magnetism.* **5** (1973) 27.
13. J. Singh and S.M. Copleyrhe (Eds), 'Novel Techniques in Synthesis and Processing of Advanced Materials', Minerals, Metals Materials Society, (1995) p. 455.